# Study of gas-liquid mixing in stirred vessel using electrical resistance tomography

**Farooq Sher[a,e*], Zaman Sajid[b,e], Begum Tokay[a], Martin Khzouz[c,e], Hamad Sadiq[d,e],**

*a School of Chemical and Environmental Engineering, University of Nottingham, Nottingham NG7 2RD, UK.*

*b. Process Engineering, Faculty of Engineering and Applied Science, Memorial University of Newfoundland, NL, A1B 3X5 Canada.*

*c. School of Mechanical, Aerospace and Automotive Engineering, Faculty of Engineering, Coventry University, Coventry CV1 5FB, UK.*

*d. Institute of Chemical Engineering and Technology, University of the Punjab, Lahore, 54590, Pakistan.*

## Abstract

This study presents a full operation and optimisation of a mixing unit; an innovative approach is developed to address the behaviour of gas-liquid mixing by using Electrical Resistance Tomography (ERT). The validity of the method is investigated by developing the tomographic images using different numbers of baffles in a mixing unit. This technique provided clear visual evidence of better mixing that took place inside the gas−liquid system and the effect of a different number of baffles on mixing characteristics. For optimum gas flow rate ($m^3$/s) and power input (kW), the oxygen absorption rate in water was measured. Dynamic gassing−out method was applied for five different gas flow rates and four different power inputs to find out mass transfer coefficient ($K_La$). The rest of the experiments with one up to four baffles were carried out at these optimum values of power input (2.0 kW) and gas flow rate ($8.5 \times 10^{-4}$ $m^3$/s). The experimental results and tomography visualisations showed that the gas−liquid mixing with standard baffling provided near the optimal process performance and good mechanical stability, as higher mass transfer rates were obtained using a greater number of baffles. The addition of single baffle had a striking effect on mixing efficiency and additions of further baffles significantly decrease mixing time. The energy required for complete

---

[*]Corresponding author. *Tel*.: +44 (0) 7472 550 250
*E-mail addresses*:Farooq.Sher@nottingham.ac.uk, Farooq.Sher@gmail.com (F.Sher)

mixing was remarkably reduced in the case of four baffles as compared to without any baffle. The process economics study showed that the increased cost of baffles installation accounts for less cost of energy input for agitation. The process economics have also revealed that the optimum numbers of baffles are four in the present mixing unit and the use of an optimum number of baffles reduced the energy input cost by 54%.

**Keywords**

Gas−liquid mixing, hydrodynamics, mass transfer, tomography, stirred vessel, baffles, and process economics.

# 1. Introduction

From customarily unit operations, mixing is one of the most important process used in engineering and allied industries, which plays an important role in the commercial success of industrial operations. Fluid mixing has been extensively studied for many years. The major applications of mixing include in chemical and biotechnological industries, where single and multi-phase fluids are mixed in stirred tanks [1]. The process scale-up, design of a mixing equipment, energy input and mixing products quality depends on the flow behaviour of a stirred tank. Therefore, an understanding of such flow pattern is important [2].

Mechanically-stirred tanks are extensively used in the chemical and process industries, including applications in the production of chemicals, pharmaceuticals, foods, paper, minerals, metals and many others [3-6]. Typical operations which are usually carried out in mixing tanks include blending of liquids, contacting of a liquid with a gas or second immiscible liquid, solids suspension and chemical reactions. Despite many years of research and accumulated experience in the design of this important type of equipment, the fluid flow behaviour of stirred tanks still remains a subject of active investigation. The design of a stirred tank needs to be carefully matched to the particular operation, but due to the complex flow patterns encountered many uncertainties remain in the design and scale-

2

up procedures. Operations involving multiphase mixtures, e.g. contacting of a liquid with a gas, another immiscible liquid, particulate solids, or some combination of these, form a large proportion of stirred tank applications. For multiphase operations, there are significant additional complexities which need to be addressed, compared with single-phase liquid flow. Many of the uncertainties in design are related to multiphase aspects, and therefore, the focus of this study is on multiphase flow. More specifically, this study considers the case of gas–liquid contacting, which takes place on a pilot scale stirred vessel.

In the design and operation of stirring tanks, mass transfer is one of the vital phenomena, where agitation and aeration are influential variables to deliver an effective rate of mass transfer during the mixing process, it can be characterised and analysed by the means of mass transfer coefficient ($K_La$). The values of $K_La$ are affected by several features, including the geometry of the tank, type of impeller, agitation speed, aeration rate, media composition and properties [7]. The determination of the $K_La$ in mixing is also crucial to baseline efficiency parameters and to quantify the optimum operating variables. The $K_La$ for gas absorption is calculated using dynamic gassing–out method [8, 9].

Many experimental studies have been undertaken over the years to investigate the characteristics of fluid flow in stirred tanks. Often, these studies have resulted in empirical correlations, which relate a global parameter, e.g. power draw, mixing time or mass transfer rate, the geometric configuration and operating conditions [10-14]. One approach for determining the details of internal flow is through experimental studies at laboratory scale. A range of advanced measurement methods [15-18] have been applied to get valuable information; whilst there are also various limitations. For example, it is very difficult to apply experimental methods to full-scale industrial tanks, and therefore, uncertainties during scale-up need to be addressed. Moreover, the experimental methods use model fluids (e.g. water and air), but real industrial processes potentially deal with fluids which show variations from ideal behaviours at high temperatures and pressures.

In recent research, the study of the flow behaviour of a system using its flow visualisation has gained momentum. Tomography is one of the many techniques, which provides the images of the contents within a closed system. The basic principle of electrical resistance tomography (ERT) is to take multiple measurements at the periphery of an equipment, vessel or pipeline and combine these to provide information on the electrical properties of the process volume. Since the mixing vessel is a closed system, ERT is implemented as a tool to investigate the mixing phenomena. ERT has also been utilised to study the mixing behaviour of gas-liquid-solid systems, fibre suspensions, pulp mixing, polymer particles mixing and many more [19-25]. But less has been written about the use of ERT to study the gas-liquid mixing phenomena [26].

In the present study, gas-liquid mixing in a mechanically stirred vessel was analysed by using ERT method. This technique applies currents or voltages and measures these parameters via electrodes fitted on the edges of the domain. The study is also novel in a sense that the effect of mixing on concentration is studied by changing the number of baffles. To determine the effectiveness of the results developed, the mixing curves were compared with the literature [27]. Moreover, a new instrumental platform for validation of optimum power and energy consumption in stirred vessel was also investigated. One of the most stimulating elements in the design is cost estimation to build and operate the system, for that process economics of the mixing unit was also studied to evaluate the power consumption, installation and operational cost.

## 2. Experimental setup

### 2.1 Mixing unit

The experimental arrangement is shown in Fig. 1. The mixing unit consisted of a transparent Plexiglas cylindrical vessel. The internal diameter (T) was 0.217 m. The vessel was filled with water up to a

height (H) of 0.217 m. To prevent vortex and dead zones, the vessel was fitted with four equally spaced PVC baffles. The baffles used had the standard width of 0.022 m (T/10) with a clearance of 0.004 m (T/50) to the vessel walls. ERT probe was constructed on one of these baffles. A standard six blades Rushton turbine impeller with a diameter (D) of 0.072 m (T/3), width B= D/5 and height W = D/4 was used. The impeller off−bottom clearance C= T/3, was measured from impeller disc centre to the bottom of the vessel. A top entering impeller assembly was fitted in the vessel. A variable frequency drive (VFD) was used to change the impeller speed up to the desired rotational speed (rpm). A rotary torque transducer E202 torque meter was installed to measure impeller speed and torque. Gas flow was supplied via a sparger mounted centrally on the base of the vessel. The Gas sparger consisted of sixteen (16) air holes; each of them had a diameter of 1 mm, which gave a total area of $1.256 \times 10^{-5}$ m$^2$ for holes. The circumference, which contained the holes, had a diameter of 0.06 m. The ring sparger was positioned at a length of T/6 from the base of the mixing vessel. In addition to this, an electrical resistance tomography system and a computer was setup on the unit. The tomography system was made by Industrial Tomography System Manchester, United Kingdom (UK).

## 2.2   Tomographic probe design and construction

The tomographic probe was constructed on one of the baffles [28-31]. The tomographic probe was made of a 35-micron tin-clad copper foil. The foil was coated with an electrically conductive acrylic adhesive. This copper foil was selected due to its removable silicone liner, which was helpful for gluing on the plastic surface, the coating acrylic adhesive was a conductive, good high and low-temperature resistance, excellent resistance to ozone, oil, chemicals and water and at last, it was easily soldered. The electrodes dimensions were a function of the velocity of materials, diameter of the vessel, conductivity range under study. The required imaging speed was a function of the vessel's diameter, conductivity range to be measured, the velocity of the fluid and the required imaging speed. A vertical series of the electrodes of equal dimensions were arranged at the same distances on one of the baffles. The total length of one electrode used was 1.5 cm with a width 6 mm. In total 18 electrodes of length 6 mm were used as a gap of 2 mm each. The electrodes were screwed and wired to the baffle, the design and actual constructed ERT probe is shown in Fig.2.

The two spare electrodes referred to as the ground or earth electrodes (one at the top and one at the bottom), which were located away from the measurement electrodes but were in electrical contact with the fluid inside the vessel. It was made sure that all measurements of voltages were fixed against a common ground source. A co-axial cable was used to connect the data acquisition system (DAS) device with electrodes, which were in contact with the fluid inside the vessels. The outer coat of the co−axial cable is buckled to the feedback path of a buffer voltage to provide noise indemnity and the inner core was capacitively coupled to the input of the voltage buffer. This reduced the electromagnetic noise and interference. After the construction of this ERT linear probe, all the electrodes are separately checked by ohms meter. They were calibrated and tested with a standard solution and found, according to the standards and gave a good quality of results [28, 29, 31]. In the contiguous approach, two adjacent pair of electrodes was used to apply current. Voltage was measured through the remaining adjacent pair of electrodes, and an injection pair of electrodes was swapped to the next pair of electrodes and was repeated until all independent combinations were completed, according to Eq. 1, for a plan of sixteen electrodes it provides one hundred and four voltage individual measurements.

$$M_e = \frac{n_e(n_e - 3)}{2} \qquad (1)$$

Where $M_e$ represents number of independent voltage measurements without those that were obtained with electrode(s), which were used for current injection and $n_e$ represents the electrodes' number. Finally, the data was processed using ITS System 2000 Version 5.0 image rehabilitation algorithm in host image reconstruction unit, which communicates through DAS. The algorithms exist in the host computer connected to the DAS and used both on- and off-line depending on the time constraints and the type of image required. The distinction between the two algorithms is that one produces images depicting a change in resistivity relative to an initially acquired set of reference data, and the other produces an image depicting the values of resistivity or conductivity for each pixel [32].

## 2.3   Experimental procedure

The air and tap water were used, as gas phase and liquid phase fluids respectively throughout all the experiments. For every experiment, the vessel was filled up with water up to a height (H), equivalent to the vessel diameter (21.7 cm). Before each experiment, the oxygen of the water was removed by means of a current of nitrogen. The flow rate of both gases was controlled by two separate installed valves. A Rotameter (METRIC 18XA) was used in the line to control and determine the rate of aeration. The concentration of dissolved oxygen in water was measured using an oxygen probe connected to bench microprocessor based logging meter (HANNA HI964400). The probe measured dissolved oxygen concentration with a sensor covered by a membrane and temperature with a built-in temperature sensor. When a voltage was applied across the sensor, the membrane allows oxygen to pass through and oxygen that had passed through the membrane caused a current flow. The air was supplied to the vessel from a combressor through a 6 mm diameter rubber piple. Before entering into the vessel, the air passed through a filter.

The data acquisition system P2000 is provided by ITS (Industrial Tomography System) was used. It had connectors to connect up to eight electrode planes, another connector for the power supply and one for the local earth was on the back. The individual plane of electrodes on the ERT sensor was connected to the device by the 36−way connectors.

Gas-liquid mass transfer measurements were performed without baffles at standard configurations; the system was fixed at four different power inputs as 1.0, 2.0, 3.0 and 5.0 kW; while air flow rates were changed as $2.6 \times 10^{-5}$, $1.0 \times 10^{-5}$, $2.4 \times 10^{-4}$, $5.0 \times 10^{-4}$ and $8.5 \times 10^{-4}$ m$^3$/s. The values of dissolved oxygen concentration were recorded at an interval of 10 s. Moreover, for each of the above pair, the mass transfer coefficients ($K_L a$) were calculated using dynamic gassing−out method [8, 9].

The power number $N_P$ is used to describe the power consumption $P$ of the stirrer. Power number depends on different factors which are mentioned in Eq. (2).

$$N_P = \frac{P}{\rho N^3 D^5} \qquad (2)$$

Where $\rho$ is the density of the container fluid; $D$ represents the impeller's diameter and $N$ refers to impeller rotational speed. Holland and Bragg (1995) revealed that with the help of Eq (3) and (4), $N_P$ can be correlated to degree of turbulence in tank, called Reynolds number $N_{Re}$, and Froude number $Fr$:

$$N_{Re} = \frac{\rho N D^2}{\mu} \qquad (3)$$

$$F_r = \frac{N^2 D}{g} \qquad (4)$$

Where $\mu$ is the fluid viscosity, $g$ is the gravitational acceleration. For a fully baffled single phase system, which is operating in the turbulent region, the effect of Froude and Reynolds numbers are dominated by inertial forces, which could be neglected. In the gassing process another important dimensionless number is the gas flow number $F_g$:

$$F_g = \frac{Q_g}{N D^3} \qquad (5)$$

Where $Q_g$ is sparger gassing rate. For the flow developing in the impeller zone, flow number is very important, which comprises the reaction of impeller diameter, rotating speed, and gassing rate but not dependent on the geometry of the blade.

## 2.4 Process economics

The cost of baffles and its installation cost was adopted from literature [33, 34]. The amount of energy input for no baffle, one, two, three and four baffles were also analysed. The amount of energy input for each case was converted into dollars spent to generate that energy. The cost data for energy input was adopted from literature [33]. Since the cost data was not updated in the reference list, the cost data was updated to the year 2014 using Chemical Engineering Plant Cost Index (CEPCI). The cost indexes for reference years were adopted from American Institute of Chemical Engineers (AIChE) website. A graphical relationship was developed to report the optimum number of baffles required for

this system. The optimisation here is referred as the minimum cost, where the system provides or start to provide higher mass transfer efficiencies.

## 3. Results and discussion

### 3.1 Hydrodynamics and gas−liquid mass transfer measurements

In order to increase the reliability of the results, all experiments were run in triplicate and the results presented are averaged of all runs performed for each case. For optimum operation, hydrodynamic and mass transfer mechanisms are important to understand the mixing inside the vessel. Upon different power inputs, various flow patterns in the vessel were observed without any gas flow. Fig. 3, shows the Power number in terms of Reynolds number, it also represents some distinctive flow patterns inside the stirred vessel with standard Ruston turbine impeller.

The Power number was measured in the range of $5 \times 10^3 < R_{Ne} < 7 \times 10^4$ over the Reynolds number also shown in Fig. 3, which displays a preliminary value of 90.8 which declines to 31.2 at a Reynolds number 15,120. Then it leftovers consistent decreasing with Reynolds number till it falls suddenly by 43% to 9.8 at a Reynolds number value equal to 26,352; afterwards it varies a little with Reynolds number, with an average value of 4.75. This rapid fall in Power number with the Reynolds number is related with the rapid flow evolution from radial to axial, which was also witnessed visually during the experiment. This specific flow evolution was also noticed by Hockey $et$ $al.$ [35]. The plotted measurement are in good agreement with the others published literature [27].

The development of the $K_La$ in terms of the gas flow rate, with various power configurations, was studied with the Rushton turbine impeller and is shown in Fig.4. The $K_La$ value boosts with rising gas flow rates due to the augmented gas holdup. The effect is more significant for lower power inputs. For 1.0 and 2.0 kW, $K_La$ value continuously increasing when the gas flow rate is increased, and reached to 0.075 and 0.085 s$^{-1}$, respectively. However, when the power inputs are set to 3.0 kW and 4.0 kW, the

9

rate of increase $K_La$ is smaller, and there is no significant change in $K_La$ value when the gas flow rate is set to $5.0\times10^{-4}$ m³/s and above.

For $4.8\times10^{-4}$ m³/s gas feed, the highest $K_La$ value of 0.080 s⁻¹ was obtained for 4.0 kW. However, at the highest gas flow rate $8.5\times10^{-4}$ m³/s, the maximum $K_La$ value of 0.085 s⁻¹ is recorded for 2.0 kW power input rather than for the highest power input 4.0 kW. Hence, the values of $K_La$ are not so sensible to the variation of the power inputs in judgement with different air flow rates. An economic performance criterion was deduced from these $K_La$ values in terms of the efficiency of the impeller at different power inputs. These optimum values of power input (2.0 kW) and gas flow rate ($8.5\times10^{-4}$ m³/s) were used in the rest of the experiments by changing the number of baffles in ERT system.

## 3.2 Effect of the number of baffles on gas–liquid mixing

The degree of mixing with a changing number of baffles under gassed condition is represented in Fig. 5. It clearly illustrates that insertion of baffles into the system can significantly improve the gas-liquid mixing with even standard Rushton turbine impeller. It was observed that without any baffle the maximum value of oxygen concentration 17.90 ppm was achieved though after 1020 s. The long duration of the oxygen concentration to reach a level of 17.90 ppm is due to none turbulence and less interfacial contact in the mixing region. Visual observations show that the tangential motion of the low viscosity liquid (water), imparted by rotating impeller has created a swirl, which has approximated solid body rotation producing inadequate mixing. Only one baffle has significantly reduced the blend time and also increases the oxygen concentration value. The oxygen concentration reached to 18.50 ppm as compared to 17.90 ppm of without baffling, which is a 3.35% increase in the maximum value of oxygen concentration.

Addition of the second baffle shows the dominant effect on oxygen concentration, which measured as 19.20 ppm. That is, as compared to 17.90 ppm of without baffling, an increase of 7.26%. The addition of the first and the second baffles has greatly decreased the blending time, whilst addition of the third baffle has minimal effect on the oxygen concentration. Fig. 5 clearly shows that in the case of two

10

baffles the maximum level of oxygen concentration was 19.20 ppm, which approaches to only 19.50 ppm in the case of three baffles, 1.68% raise as compared to two baffles. The time to achieve the maximum level of oxygen concentration was 610 s when two baffles were employed, whereas it was recorded as 590 s for three baffles. Furthermore, the addition of the fourth baffle achieved highest oxygen concentration (19.98 ppm), which corresponds to 11.6% increase in concentration from no baffle value (17.9 ppm). Also, the highest level of oxygen concentration was achieved in the shortest time 510 s. In the case of four baffles, system vortex formation was completely eliminated and the swirling motion was converted into the axial flow, which helps to achieve the maximum mass transfer and greater mechanical stability in gas–liquid mixing. Hence, by increasing the number of baffles break swirling and vortexing of liquid inside the vessel, and increase mixing and stabilizes the power drawn by reducing mixing time. Myers, Reeder *et al.* [36] predicted similar results output, while gas–liquid mixing in the study on optimise mixing by using the proper baffles.

## 3.3    ERT for evaluating gas–liquid mixing

In contemplation to get a more in-depth understanding about the gas-liquid mixing, ERT technique was used, which usually show the dispersal of the conductivity inside the mixing unit. The use of different colours combination helps to interpret the conductivity or eventually gas absorption in a specific area of the vessel [37]. In the present study, the gas phase oxygen (in air) was a conductive and liquid phase (tap water) was non-conductive without any dissolved oxygen. A typical set of tomograms was obtained using this technique which is shown in Fig. 6. These are based on the experiments conducted at an optimum power of 2.0 kW and gas flow rate of $8.5 \times 10^{-4}$ m$^3$/s with various numbers of baffles.

Each image is collected when the contents of the mixing were at steady state and is an average of several images together. The data collection time for a single image is around 30 ms. The tomographic image comprises 20×10 pixels, which gives electrical conductivity dissemination information in both axial and radial directions. The accumulation of oxygen and its dispersal all over

the sensing volume as the agitation rate increased was clearly identified. The blue colour shows background water, while the green colour represents low conductivity (less oxygen concentration) and red−yellow colour depicts high conductivity (more oxygen concentration) in the water.

Fig. 6(a) shows background measurement with the addition of one baffle, blue and green regions represent the distribution of very low electrical conductivity, reflecting the less dissolved oxygen within the sensing volume, it is also evident from Fig. 5 even after 1020 s the maximum oxygen concentration detected was 17.90 ppm. Fig. 6(b) images confirm that the addition of the second baffle to the vessel visibly identified; as the agitation is increased the deep blue colour is swapped by a red− yellow with time showing that the oxygen has well mixed within the sensing volume. As seen in Fig. 6(b) and (c), there is not a significant difference between the pixels of the tomography images with two and three baffles, oxygen concentration increased only 0.30 ppm by changing two to three baffles. Fig. 6(d) represents the addition of the fourth baffle, which made a significant effect on mixing and the blue colour shade is completely replaced by red−yellow colour, even at the early stages, showing higher conductivity in terms of higher dissolved oxygen concentration in the vessel, reaching a maximum value of 19.98 ppm which is also shown in Fig. 5. This proves that there are less dead zones present in the case of four baffles as compared to one baffle. The results indicate that there is proper mixing by the use of a higher number of baffles.

For further more evidence, the conductivity data recorded during the experiments was also analysed and presented in Fig. 7, which indicate that conductivity values increase upon the oxygen absorption in the water.

Conductivity value increased from 0.297 S/m to 0.301 S/m with the addition of one baffle. Upon addition of the second and third baffle, the conductivity values of 0.302 S/m and 0.303 S/m were noticed respectively, which is a 0.3% addition to the value as compared to once baffle, which was 1.3%. It is also evident from Fig. 5 that only the first baffle makes the significant difference in oxygen

concentration in the mixing unit. A maximum conductivity value of 0.305 S/m was recorded with all four baffles, which is a 0.6% addition as compared to no baffling system.

## 3.4 Optimisation and process economics

### 3.4.1 Gassed to un-gassed power measurements

The gassed to un-gassed power ratio, *Pg/P* is plotted against the gas flow number, *Fg* for Rushton turbine impeller shown in Fig. 8. Increasing gas flow rate *Qg* from 0 to $8.5 \times 10^{-4}$ induce a fall in the *Pg/P* ratio values from 1.0 to 0.4.

For small gas flow rate, a sudden decrease (about 20%) occurs at *Fg* value of 0.02, whereas for medium gas flow rate this decrease in the ratio of the *Pg/P* is comparatively slow. Lately at *Fg* value of 0.07 and above an average decrease of about 4.4% in the ratio of *Pg/P* was observed; which ends up with *Pg/P* value of 0.4 against *Fg*, 0.17. This fall in *Pg/P* with rising gas flow *Qg* was linked with the evolving size of the gas occupied voids around the impeller blades, which has been comprehensively stated in the literature [26]. The power curve obtained is consistent with the one in the literature [27, 38]. The consistency of the power curve of the current study with literature shows that the methodology adopted to study gas-liquid mixing has valid applications in this area.

### 3.4.2 Power consumption and system efficiency

The cost of a gas-liquid mixing process mainly contingent on the power consumption. In order to make sure the best productivity, energy consumption must be optimised. The efficiency of the system could be defined as the function of gas concentrations and blend times [39]. Hence, the efficiency of the mixing unit is calculated from the time taken to achieve 17.90 ppm of oxygen concentration without and with different number of baffles.  Fig. 9 depicts, even with only one baffle, time; 400 s spent was almost 1/3rd of the time when there was no baffle for mixing. The same amount of oxygen concentration was reached in 340 s with two and 320 s with three baffles, which is 67% and 73% improvement in the system efficiency, respectively. The system efficiency was 100%, while same concentration was reached in just 290 s for four baffles. With the addition of one, two, three and four

baffles the system efficiency increased up to 50%, 67%, 73% and 100%, respectively, as compared to zero baffle system as the same level of performance is achieved in much shorter time.

The energy of the system is determined by using simple multiplication of operative power value with the time taken for complete mixing. As the number of baffles increased less energy is required to achieve maximum oxygen concentration. The energy requirement for complete mixing was 408 kJ in the case of no baffles. When the first baffle was introduced into the system, the consumption reduced to 272 kJ. Similarly, after the addition of the second and the third baffle the energy consumption was decreased to 244 kJ and 236 kJ which is about 70% increase in system efficiency. In the case of four baffles system's energy needed is measured as half. In short, as the extent of baffling in the system is increased, from un−baffled to one, two, three and four standard baffles, the energy requirement continually decreases and energy saving increases.

An economic analysis has also been applied to the current mixing unit and the results are presented in Fig. 10, which displays the influence of number of baffles on the cost of the baffles and the cost of energy input for the system. The cost of baffle here represents the cost of baffle plus its installation cost. With no baffle, the system requires high-energy input with which a high cost of energy production is associated as more power is required to mix the contents properly. In this case, there was no cost of the baffle. However, the energy input was the highest and same as its cost which was $119. The introduction of one baffle introduced its cost into the system. The presence of this baffle helped to save a significant amount of the cost of energy input. The cost of the baffle was increased from $0 to $30, whereas the cost of energy input was decreased from $119 to $40. This introduced an increase of $30 and a decrease of $79 – a net saving of $49 for each unit of energy input. The use of the second baffle further lowered the cost of energy input by $20. However, the cost of the baffle has increased to $62. Similarly, by increasing the number of baffles, the cost of baffles was increased. However, the cost of energy input was decreased significantly up to the fourth baffle as optimum mass transfer rates and mixing time was achieved at four numbers of baffles and less energy was required to obtain the same mass transfer rate.

In this economic analysis, the capital needed for the installation of baffles is the start-up capital and is the one-time expense only, whereas the cost of energy input is categorised as operating capital. With a maximum number of baffles, the cost of energy input is $55 and the baffles cost is $100. If the unit is made to operate for 20 hours a day, the operating cost would be $1100 and the capital cost would be $100. For no baffles, the cost of energy input is $119 and the cost of baffles is $0. This predicts an operating cost of $2380 per day. Thus, the introduction of four baffles provides a total cost reduction of $1280 per day. The results obtained are similar to the ones in the literature [40-42].

This part of paper studies the bare costs associated with liquid-gas mixing unit. However, the previous economic analysis in literature studies the full cost of mixing unit installation, scale-up of unit, cost of liquid in the vessel, the size of the plant, the cost associated with the mechanical failure of the unit (mechanical reliability failure) and maintenance cost, which we consider out of scope for the current study. Fig. 10 should also be analysed with the fact that the installation of baffles is a fixed-capital investment, once installed the system will provide a good mixing until its valuable life. Moreover, the cost of energy consumption is an operational cost. The study shows that a fixed-capital investment can save an amount of money, in terms of lowering the operational cost. The optimisation analysis shows that the minimum numbers of baffles required for the system are two, though this result depends on the dimensions of mixing tank under study.

## 4. Conclusions

In this study, a major area of gas–liquid mixing was studied. It can be concluded that the tomography has the potential to be used as a modelling tool and diagnostic tool. This is also a general method of finding out what is occurring in process vessels. The ERT probe has been designed, manufactured and successfully tested, which can be used for the gas–liquid mixing analysis in stirred vessels and tanks routinely. The visualisation of the gas–liquid mixing in dynamic mixing has shown the behaviour of two different phases in the mixing vessel. The complete mixing process by adding the gas, its

dispersion until it reaches the equilibrium concentration has been undertaken using the ERT. The qualitative information on the flow and dispersion rates has been obtained by using different numbers of baffles through images at different times in the mixing vessel. The effects of vortex and number of baffles on the gas−liquid mixing rates have been analysed. The best mixing in shorter time was found while using four baffle systems. The energy consumed for full mixing was reduced to 204 kJ with 100% system efficiency in terms of four baffles. The study also concluded that the operational cost would be at a minimum if the fixed capital investment is higher for the system.  It is concluded from the observations that the use of four baffles optimises the process of mixing and the mixing can be completed with the shortest time and less operational cost. An economic analysis revealed that the use of an optimum number of baffles saved a cost of $1280 per day. More than four baffles could give better results, hence it is recommended as a future work to use more than four baffles to find out the system performance. It is recommended to perform the mixing analysis using different temperature conditions inside the mixing unit and a model may be developed to see this effect on process economics. It is also suggested to perform such economic analysis with detailed cost analysis, keeping the factors, mentioned in economic analysis part, under considerations.

# Nomenclature

$K_{La}$    mass transfer coefficient

$N_P$    power number

$Fr$    froude number

$Fg$    gas flow number

$N_{Re}$    reynolds number

$\rho$    fluid density (kg m$^{-3}$)

$\mu$    fluid viscosity (kgm$^{-2}$s$^{-1}$)

$Q_g$    gas flow rate (m$^3$ s$^{-1}$)

$g$    acceleration of gravity (m s$^{-2}$)

$T$    tank diameter (m)

$H$    liquid height (m)

$D$    impeller diameter (m)
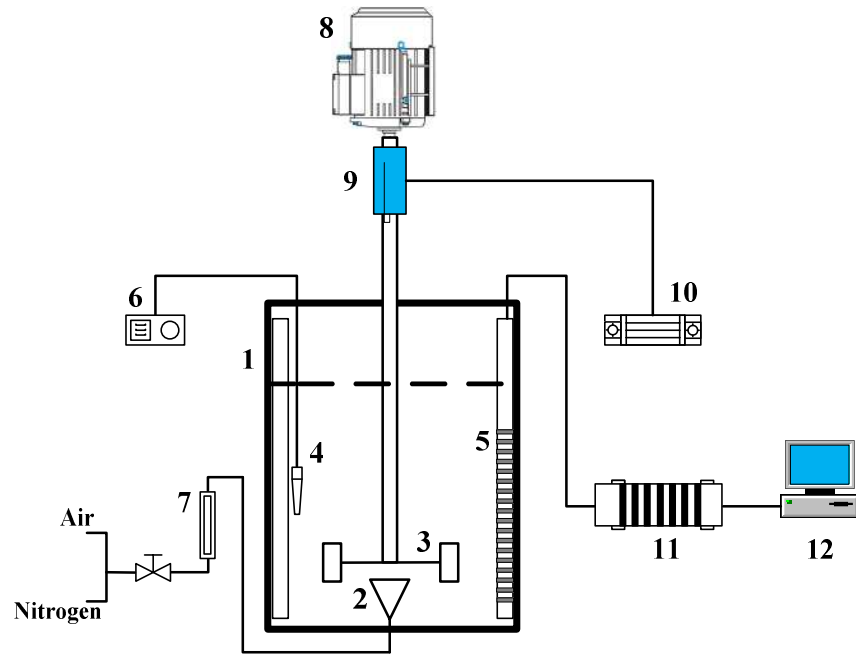
$W$    blade width (m)

$N$    impeller speed (s$^{-1}$)

**Fig. 1.** Experimental setup: 1) Stirred vessel, 2) Gas sparger, 3) Impeller, 4) Oxygen probe, 5) ERT probe and baffle, 6) Oxygen meter, 7) Rotameter, 8) Electric motor, 9) Torque meter assembly, 10) Transducer, 11) Data acquisition system ITS, 12) Computer.
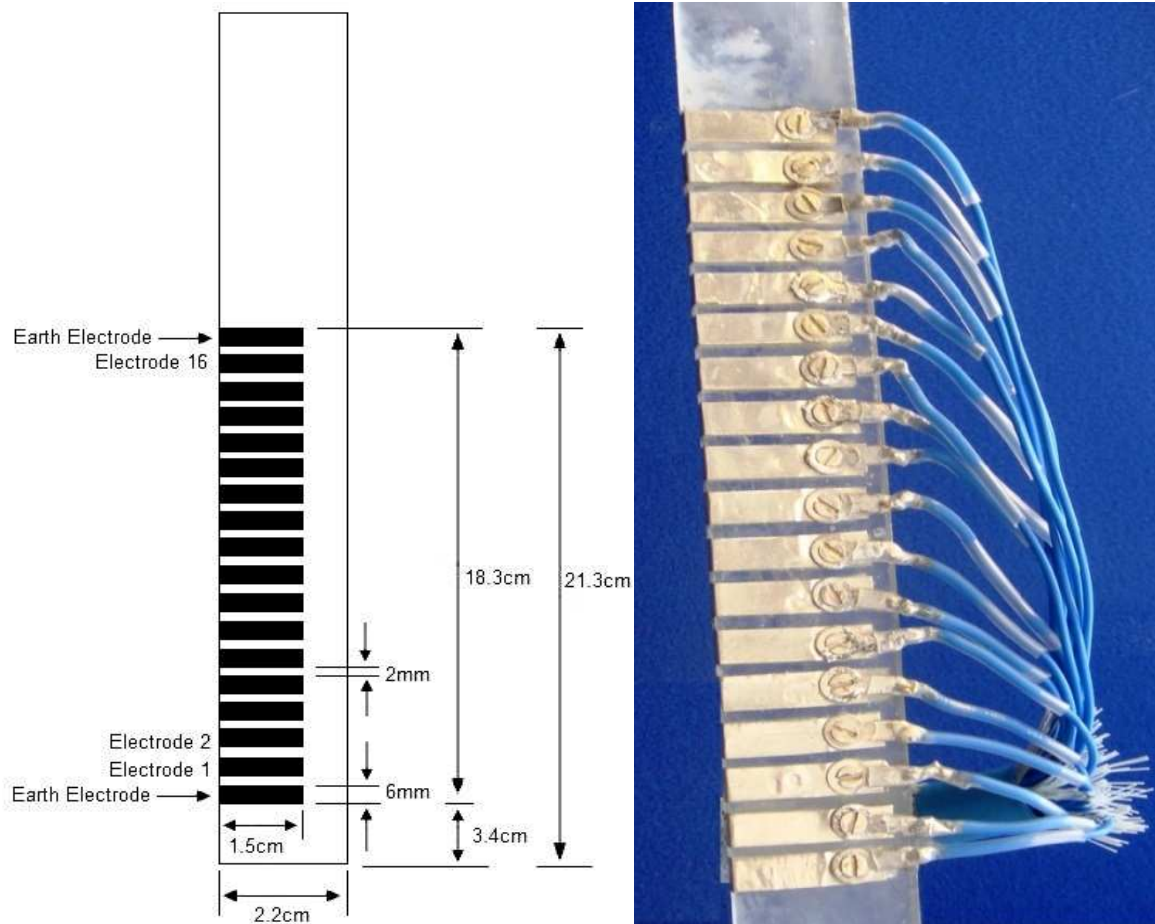
**Fig. 2.** Designed and constructed linear ERT probe.
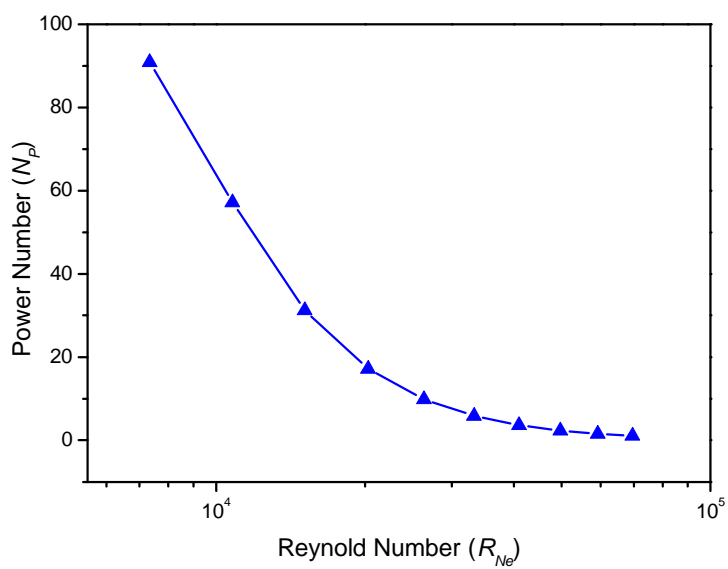


**Fig. 3.** Power number versus Reynolds number in the gas-liquid system using a Rushton turbine impeller.
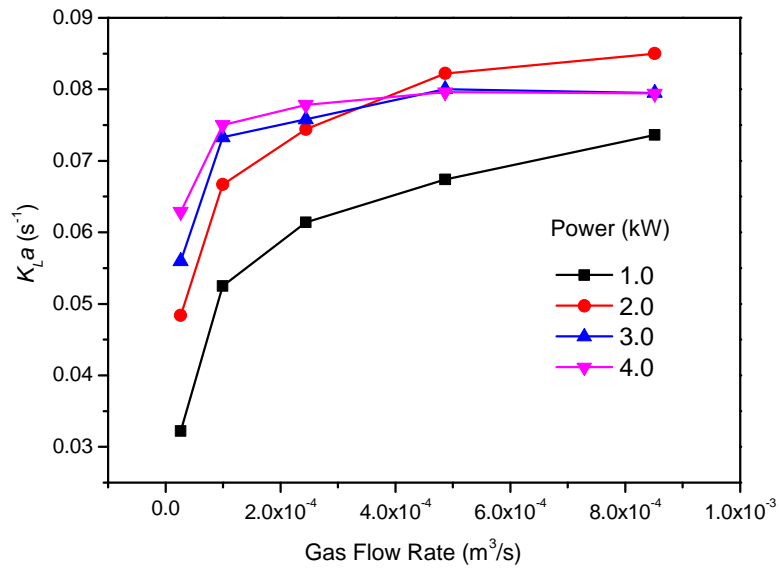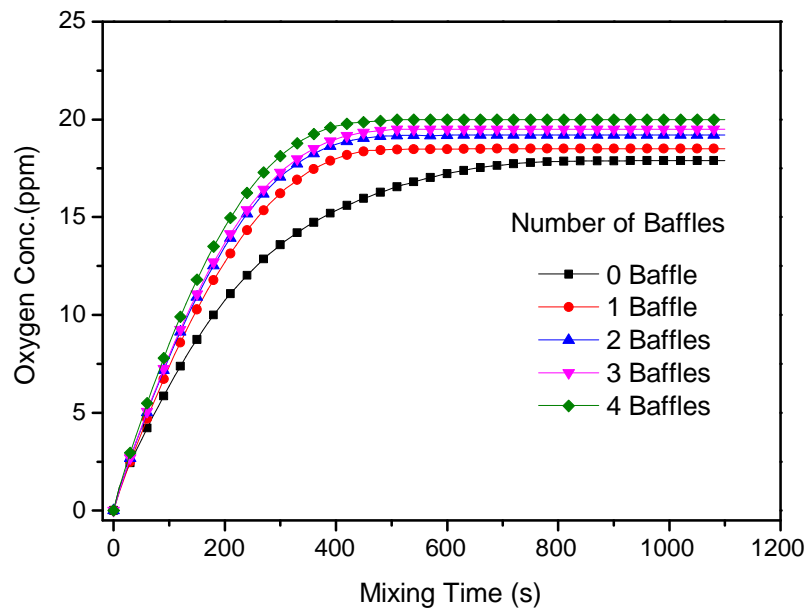
**Fig. 4.** $K_La$ values at various power and gas flow rates.



**Fig. 5.** Oxygen concentration against time with and without baffles in the mixing system.
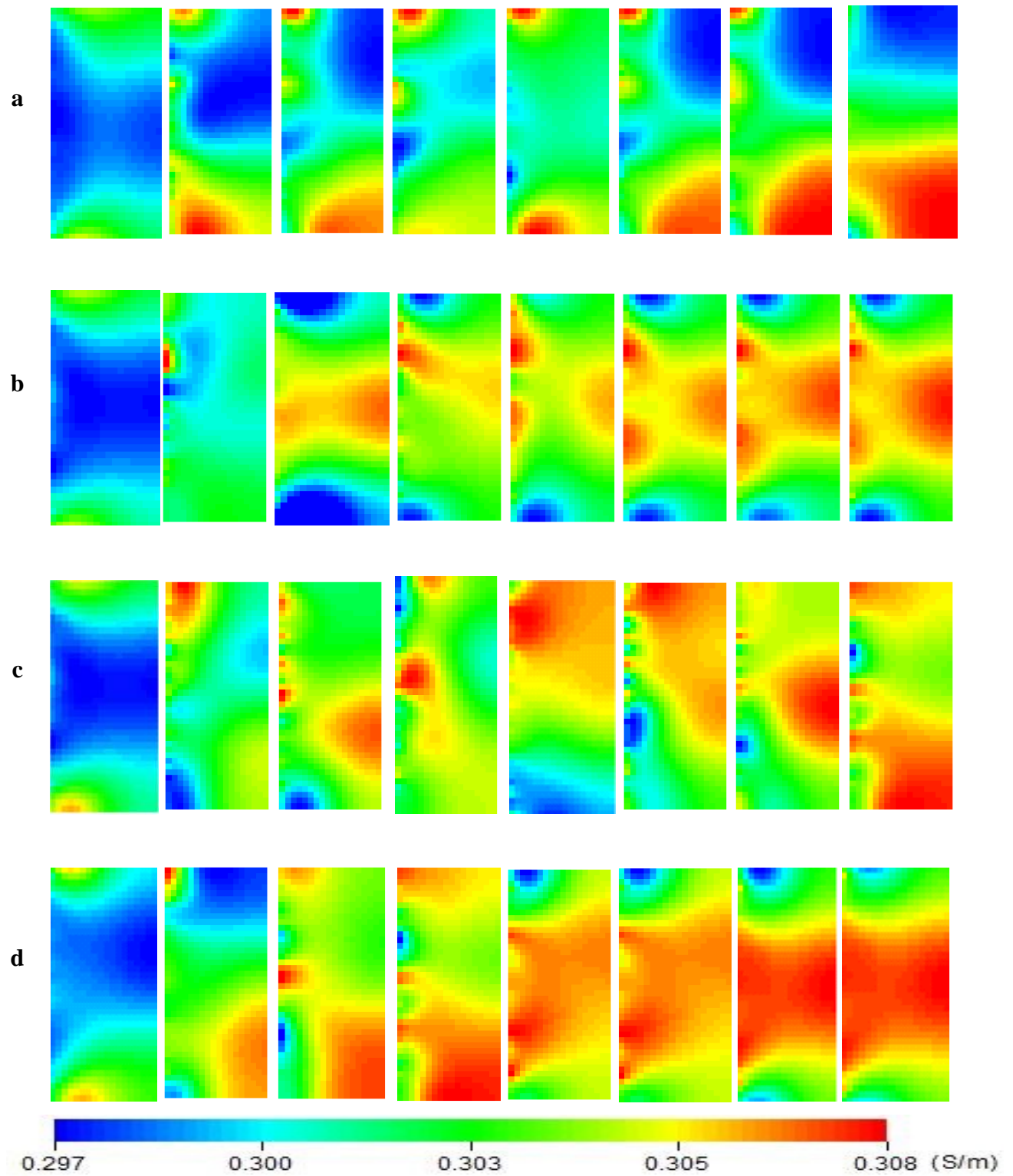
**Fig. 6.** Comparison of tomographic images with a) one, b) two, c) three and d) four baffles during gas-liquid mixing at the optimum power of 2.0 kW and gas flow rate $8.5 \times 10^{-4}$ m$^3$/s.
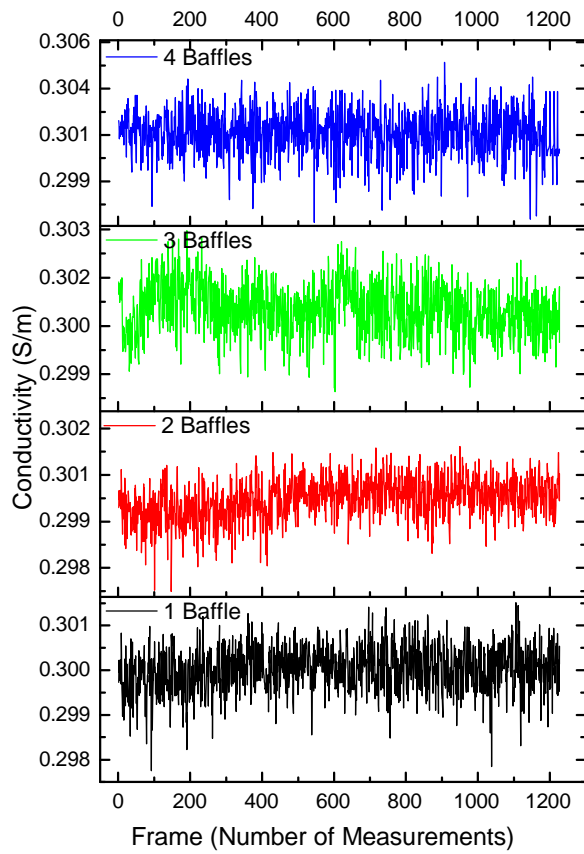
21

**Fig. 7.** Conductivity planes against the number of measurements with one, two, three and four baffles.
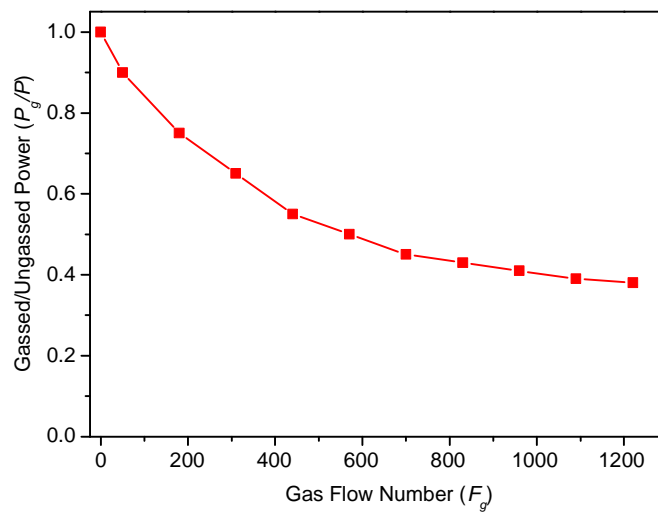


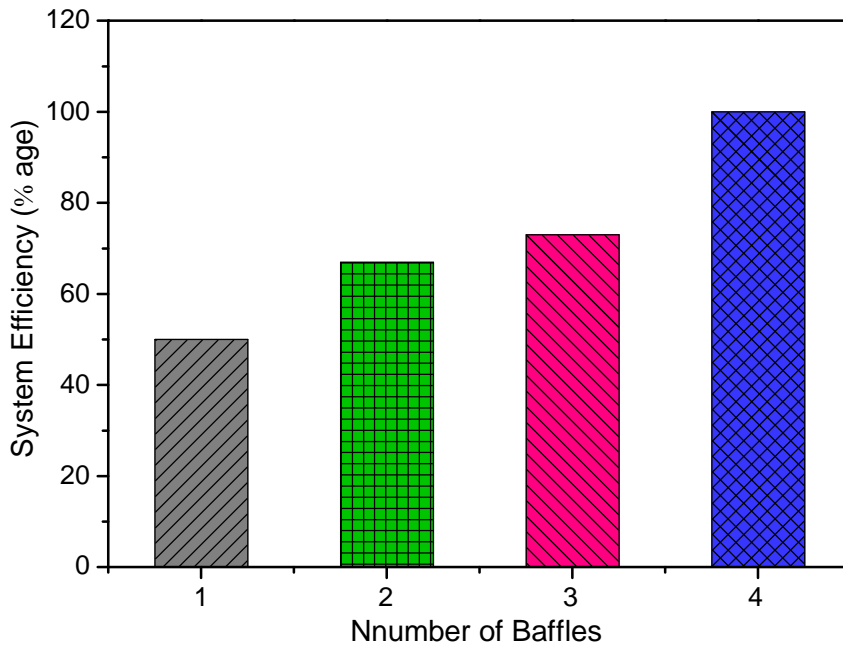**Fig. 8.** Evaluation of the gassed to un-gassed power ratio with rising gas flow rate.

**Fig. 9.** Improving mixing unit efficiency by increasing the number of baffles.
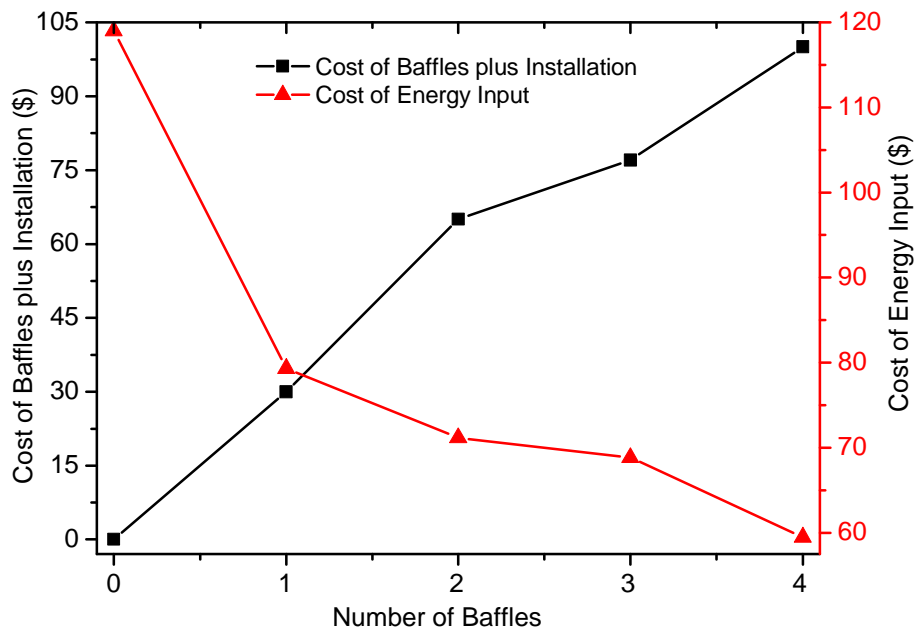


**Fig. 10.** Cost analysis of the gas-liquid mixing unit.

# References

1. Kleerebezem, R. and M.C. van Loosdrecht, Mixed culture biotechnology for bioenergy production. Current opinion in biotechnology, 2007. **18**(3): p. 207-212.
2. Paul, E.L., V.A. Atiemo-Obeng, and S.M. Kresta, Handbook of industrial mixing: science and practice. 2004: John Wiley & Sons.
3. Moinfar, S. and M.-R.M. Hosseini, Development of dispersive liquid–liquid microextraction method for the analysis of organophosphorus pesticides in tea. Journal of hazardous materials, 2009. **169**(1): p. 907-911.
4. Assirelli, M., et al., Macro-and micromixing studies in an unbaffled vessel agitated by a Rushton turbine. Chemical Engineering Science, 2008. **63**(1): p. 35-46.
5. Lane, G., M. Schwarz, and G. Evans, Numerical modelling of gas–liquid flow in stirred tanks. Chemical Engineering Science, 2005. **60**(8): p. 2203-2214.
6. Micheletti, M., et al., Fluid mixing in shaken bioreactors: Implications for scale-up predictions from microlitre-scale microbial and mammalian cell cultures. Chemical Engineering Science, 2006. **61**(9): p. 2939-2949.
7. Kapic, A. and T. Heindel, Correlating gas-liquid mass transfer in a stirred-tank reactor. Chemical Engineering Research and Design, 2006. **84**(3): p. 239-245.
8. Tribe, L., C. Briens, and A. Margaritis, Determination of the volumetric mass transfer coefficient (kLa) using the dynamic "gas out–gas in" method: Analysis of errors caused by dissolved oxygen probes. Biotechnology and bioengineering, 1995. **46**(4): p. 388-392.
9. Moutafchieva, D., et al., Experimental determination of the volumetric mass transfer coefficient. Journal of Chemical Technology & Metallurgy, 2013. **48**(4).
10. Wang, F. and Z.-S. Mao, Numerical and experimental investigation of liquid-liquid two-phase flow in stirred tanks. Industrial & engineering chemistry research, 2005. **44**(15): p. 5776-5787.
11. Lane, G., M. Schwarz, and G. Evans, Predicting gas–liquid flow in a mechanically stirred tank. Applied Mathematical Modelling, 2002. **26**(2): p. 223-235.
12. Yapici, K., et al., Numerical investigation of the effect of the Rushton type turbine design factors on agitated tank flow characteristics. Chemical Engineering and Processing: Process Intensification, 2008. **47**(8): p. 1340-1349.
13. Lamberto, D., et al., Using time-dependent RPM to enhance mixing in stirred vessels. Chemical Engineering Science, 1996. **51**(5): p. 733-741.
14. Kresta, S.M. and P.E. Wood, The flow field produced by a pitched blade turbine: characterization of the turbulence and estimation of the dissipation rate. Chemical Engineering Science, 1993. **48**(10): p. 1761-1774.
15. Adrian, R.J., Twenty years of particle image velocimetry. Experiments in Fluids, 2005. **39**(2): p. 159-169.
16. Roehle, I., et al., Recent developments and applications of quantitative laser light sheet measuring techniques in turbomachinery components. Measurement Science and Technology, 2000. **11**(7): p. 1023.
17. Schäfer, M., M. Höfken, and F. Durst, Detailed LDV measurements for visualization of the flow field within a stirred-tank reactor equipped with a Rushton turbine. Chemical Engineering Research and Design, 1997. **75**(8): p. 729-736.
18. Pettersson, M. and Å.C. Rasmuson, Hydrodynamics of suspensions agitated by pitched-blade turbine. AIChE journal, 1998. **44**(3): p. 513-527.
19. Carletti, C., et al., Analysis of solid concentration distribution in dense solid–liquid stirred tanks by electrical resistance tomography. Chemical Engineering Science, 2014. **119**: p. 53-64.
20. Aw, S.R., et al., Electrical resistance tomography: A review of the application of conducting vessel walls. Powder Technology, 2014. **254**: p. 256-264.
21. Yenjaichon, W., et al., Mixing quality in low consistency fibre suspensions downstream of an in-line mechanical mixer measured by electrical resistance tomography. Nordic Pulp and Paper Research Journal, 2014. **29**(3): p. 392-400.

22.	Abdullah, B., et al., Electrical resistance tomography-assisted analysis of dispersed phase hold-up in a gas-inducing mechanically stirred vessel. Chemical Engineering Science, 2011. **66**(22): p. 5648-5662.

23.	Yenjaichon, W., et al., Assessment of mixing quality for an industrial pulp mixer using electrical resistance tomography. The Canadian Journal of Chemical Engineering, 2011. **89**(5): p. 996-1004.

24.	Tahvildarian, P., et al., Using electrical resistance tomography images to characterize the mixing of micron-sized polymeric particles in a slurry reactor. Chemical Engineering Journal, 2011. **172**(1): p. 517-525.

25.	Hosseini, S., et al., Study of solid–liquid mixing in agitated tanks through electrical resistance tomography. Chemical Engineering Science, 2010. **65**(4): p. 1374-1384.

26.	Hari-Prajitno, D., et al., Gas-liquid mixing studies with multiple up-and down-pumping hydrofoil impellers: Power characteristics and mixing time. The Canadian Journal of Chemical Engineering, 1998. **76**(6): p. 1056-1068.

27.	Coulson, J.M., et al., Coulson and Richardson's Chemical Engineering Volume 1 - Fluid Flow, Heat Transfer and Mass Transfer (6th Edition). 1999, Elsevier.

28.	Dickin, F. and M. Wang, Electrical resistance tomography for process applications. Measurement Science and Technology, 1996. **7**(3): p. 247.

29.	Mann, R., et al. Resistance tomography imaging of stirred vessel mixing at plant scale. in Institution of chemical engineers symposium series. 1996. Hemsphere publishing corporation.

30.	Beck, M.S., Process tomography: principles, techniques and applications. 1995: Butterworth-Heinemann.

31.	Gladden, L., Process Tomography: Principles, Techniques and Applications. Measurement Science and Technology, 1997. **8**(4).

32.	Mann, R., et al., Application of electrical resistance tomography to interrogate mixing processes at plant scale. Chemical Engineering Science, 1997. **52**(13): p. 2087-2097.

33.	Peters, M.S. and K.D. Timmerhaus, Plant design and economics for chemical engineers. 2002, New York: McGraw-Hill.

34.	Towler, G.P. and R.K. Sinnott, Chemical engineering design: principles, practice, and economics of plant and process design. 2013: Elsevier.

35.	Hockey, R. and J. Nouri, Turbulent flow in a baffled vessel stirred by a 60 pitched blade impeller. Chemical Engineering Science, 1996. **51**(19): p. 4405-4421.

36.	Myers, K.J., M.F. Reeder, and J.B. Fasano, Optimize mixing by using the proper baffles. Chem. Eng. Prog, 2002. **98**(2): p. 42-47.

37.	Wang, M., et al., Measurements of gas–liquid mixing in a stirred vessel using electrical resistance tomography (ERT). Chemical Engineering Journal, 2000. **77**(1): p. 93-98.

38.	Sardeing, R., et al., Gas–Liquid Mass Transfer: Influence of Sparger Location. Chemical Engineering Research and Design, 2004. **82**(9): p. 1161-1168.

39.	Nienow, A.W., M.F. EDWARDS, and N. Harnby, Mixing in the process industries. 1997: Butterworth-Heinemann.

40.	Nienow, A.W., M.F. Edwards, and N. Harnby, eds. Mixing in the Process Industries. second ed. 1997, Butterworth Heinemann.

41.	Kenney, W.F., Energy Conservation in the Process Industries. Elsevier Science.

42.	Gubanov, O. and L. Cortelezzi, On the cost efficiency of mixing optimization. Journal of Fluid Mechanics. **692**: p. 112-136.